JACS
JOURNAL OF THE AMERICAN CHEMICAL SOCIETY

Article

pubs.acs.org/JACS

Chemical Approach to Positional Isomers of Glucose–Platinum Conjugates Reveals Specific Cancer Targeting through Glucose-Transporter-Mediated Uptake *in Vitro* and *in Vivo*

Malay Patra, Samuel G. Awuah, and Stephen J. Lippard*

Department of Chemistry, Massachusetts Institute of Technology, Cambridge, Massachusetts 02139, United States

Supporting Information

ABSTRACT: Glycoconjugation is a promising strategy for specific targeting of cancer. In this study, we investigated the effect of D-glucose substitution position on the biological activity of glucose–platinum conjugates (Glc-Pts). We synthesized and characterized all possible positional isomers (C1α, C1β, C2, C3, C4, and C6) of a Glc-Pt. The synthetic routes presented here could, in principle, be extended to prepare glucose conjugates with different active ingredients, other than platinum. The biological activities of the compounds were evaluated both *in vitro* and *in vivo*. We discovered that varying the position of substitution of D-glucose alters not only the cellular uptake and cytotoxicity profile but also the GLUT1 specificity of resulting glycoconjugates, where GLUT1 is glucose transporter 1. The C1α- and C2-substituted Glc-Pts (**1α** and **2**) accumulate in cancer cells most efficiently compared to the others, whereas the C3-Glc-Pt (**3**) is taken up least efficiently. Compounds **1α** and **2** are more potent compared to **3** in DU145 cells. The α- and β-anomers of the C1-Glc-Pt also differ significantly in their cellular uptake and activity profiles. No significant differences in uptake of the Glc-Pts were observed in non-cancerous RWPE2 cells. The GLUT1 specificity of the Glc-Pts was evaluated by determining the cellular uptake in the absence and in the presence of the GLUT1 inhibitor cytochalasin B, and by comparing their anticancer activity in DU145 cells and a GLUT1 knockdown cell line. The results reveal that C2-substituted Glc-Pt **2** has the highest GLUT1-specific internalization, which also reflects the best cancer-targeting ability. In a syngeneic breast cancer mouse model overexpressing GLUT1, compound **2** showed antitumor efficacy and selective uptake in tumors with no observable toxicity. This study thus reveals the synthesis of all positional isomers of D-glucose substitution for platinum warheads with detailed glycotargeting characterization in cancer.

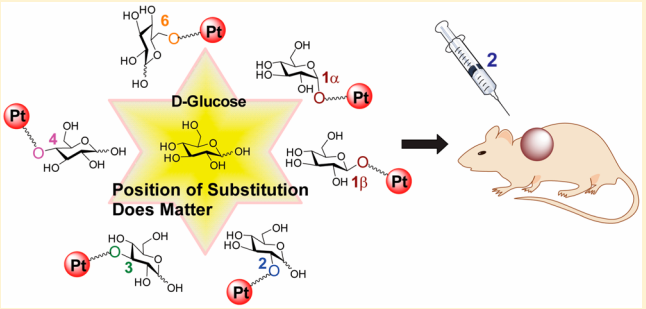

INTRODUCTION

The essential nutrient D-glucose is the main carbon and energy source for cells. Cellular uptake of D-glucose is mediated by membrane-bound glucose transporters which are classified into two main families: facilitative (GLUTs) and sodium dependent (SGLTs).[1] GLUTs transport D-glucose by an energy-independent facilitative diffusion process, whereas SGLTs-mediated D-glucose uptake is an active and energy-dependent process. There are 14 human GLUTs discovered to date, among which only GLUT1–GLUT4 have been extensively studied.[1,2] The molecular structures of human GLUT1 and GLUT3 have been reported very recently.[2,3] GLUT1 is broadly overexpressed in various cancers, including hepatic, pancreatic, breast, esophageal, brain, renal, lung, cutaneous, colorectal, endometrial, ovarian, and cervical.[1,4] GLUT1 expression levels in patient-derived tumor samples correlate well with poor prognosis.[1,4−6] Moreover, overexpression of other glucose transporters, such as GLUT2 (gastric, breast, colon, and liver carcinomas), GLUT3 (B-cell non-Hodgkin's lymphoma), GLUT12 (prostate adenocarcinomas), and SGLT1–2 (colorectal and metastatic lung carcinomas), has also been reported for certain types of cancers.[1,4,7,8]

D-Glucose is metabolized oxidatively in the mitochondria of healthy non-cancerous cells and produces 36 mol of ATP per mole of glucose. In contrast, cancer cells metabolize glucose by aerobic glycolysis, which is energetically very inefficient and provides only 4 mol of ATP from 1 mol of glucose.[9] Therefore, the rapid growth and proliferation of cancer cells demand drastic increases in glucose uptake and metabolite flux; this phenomenon is known as the "Warburg effect".[10] The altered glucose intake and glucose transporter overexpression are common in cancers and provide clinically validated targets for cancer treatment.[11−13] Over the years, the design of glycoconjugates to exploit the overexpressed glucose transporters for specific delivery of various organic anticancer drugs, fluorophores, and radiotracers to cancer tissues has been a field of active research.[14−20] The potential of glycoconjugation as a strategy in diagnosis and therapy is supported by GLUTs-mediated

Received: July 5, 2016
Published: August 27, 2016

DOI: 10.1021/jacs.6b06937
J. Am. Chem. Soc. 2016, 138, 12541−12551

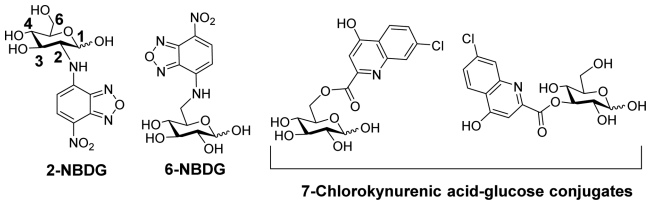

Figure 1. Representative examples of positional isomers of D-glucose conjugates having different biological properties.

uptake and selective accumulation of the radiolabeled glucose derivative ^{18}F-FDG in cancer tissues. The tracer is frequently employed in the clinic for diagnosis and staging of various types of cancers.[12,21] As an alternative to the radioisotope-labeled glucose bio-probes, various fluorescent-tagged glucose molecules were also developed.[15] Glycoconjugates of various anticancer drugs such as paclitaxel, adriamycin, and azomycin have been synthesized for specific delivery to cancer cells.[14] In order to introduce tumor-targeting properties to platinum and other metal-based anticancer compounds, we and others have reported the synthesis and biological activities of glucose conjugates of metal complexes.[22−27]

Since the introduction of glufosfamide in 1995,[28] the first explicitly designed glucose conjugate of a DNA alkylating agent ifosfamide, which exploits the overexpressed glucose transporters in the membrane of cancer cells, there has been a significant body of work on glycoconjugates in the literature.[14,15,26,29−31] However, in the past two decades, there has not been even a single report describing the synthesis of a complete set of positional isomers (i.e., C1−C6 with the same linker length) of a given glycoconjugate to investigate the influence of position of substitution in D-glucose on its biological activity. There are one primary and four secondary hydroxyl groups in D-glucose, which offer the possibility to attach a warhead or a sensor, such as a fluorophore. During the transporter-mediated translocation, these "hydroxyl" groups play important roles in hydrogen bonding interactions with various amino acid residues of GLUTs, as revealed recently in crystal structures of D-glucose-bound GLUT1 and GLUT3.[2,3] Therefore, the recognition and translocation efficiencies through the glucose transporters are expected to vary for different positional isomers of a glycoconjugate.[14] In fact, analyzing the results from a few earlier studies revealed that the position of substitution of D-glucose influences the biological properties of glucose conjugates.[14,15,30,32,33] The C6-substituted glucose conjugate of 4-nitrobenzofurazan (6-NBDG, Figure 1) binds to GLUT1 transporters with a 300-fold greater affinity than D-glucose, and that is why the rate of cellular uptake of 6-NBDG is relatively slow and not reduced efficiently by D-glucose in a competition assay.[30,34] On the other hand, its C2-positional isomer (2-NBDG, Figure 1) accumulates readily in cells, and its uptake can be inhibited efficiently when co-incubated with D-glucose.[15,35] Moreover, 2-NBDG, but not 6-NBDG, enters the glycolytic pathway in cells and is converted to its non-fluorescent 6-phosphate derivative, thereby offering the ability to study the cellular metabolic events.[15] The C6 positional isomer of a glucose conjugate of 7-chlorokynurenic acid showed superior protective activity, compared to its C3-positional isomer, against seizures induced by *N*-methyl-D-aspartate (NMDA) in mice (Figure 1).[33] Thus, syntheses and a systematic study of biological activities of various positional isomers of a given glycoconjugate are highly desirable for they might shed light on identifying the appropriate "hydroxyl" group of D-glucose at which to attach a warhead, thereby contributing to the design of next generation glycoconjugates.[14] Toward this goal, we synthesized positional isomers of glucose−platinum conjugates using [(*trans*-1,2-diaminocyclohexane)(2,2-dimethyl malonato)Pt(II)] (**7**) as the warhead (Figure 2). Biological studies revealed that the position of substitution is an important determinant of cellular uptake, cytotoxicity, and GLUT1 specificity of a glucose−drug conjugate.

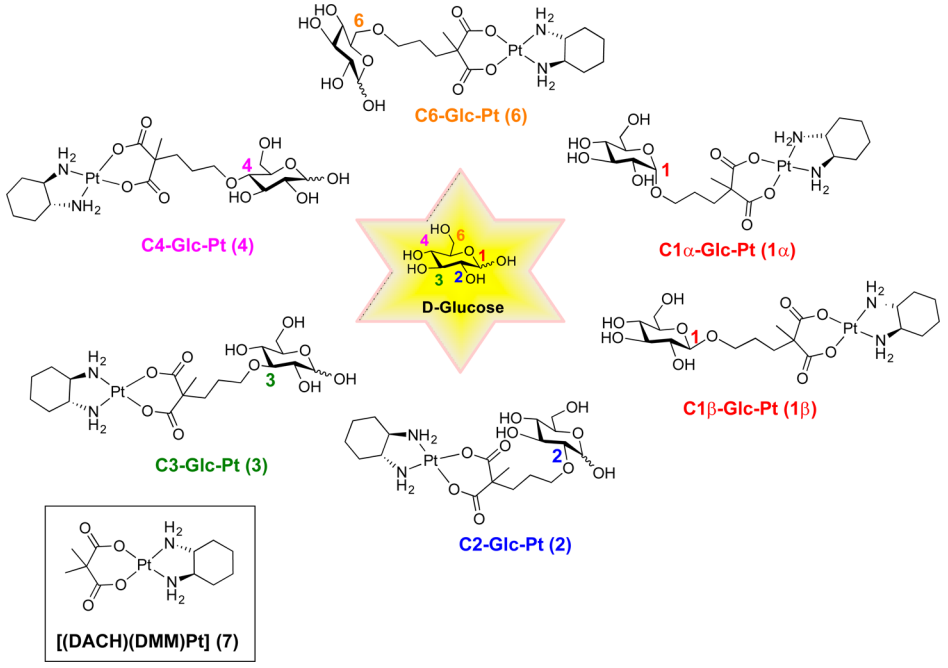

Figure 2. Structures of C1−C6-substituted positional isomers (**1**−**6**) of a glucose−platinum conjugate and aglycone **7**.

DOI: 10.1021/jacs.6b06937
J. Am. Chem. Soc. 2016, 138, 12541−12551

Scheme 1. Synthesis of C1-Glc-Pts 1β and 1α[a]

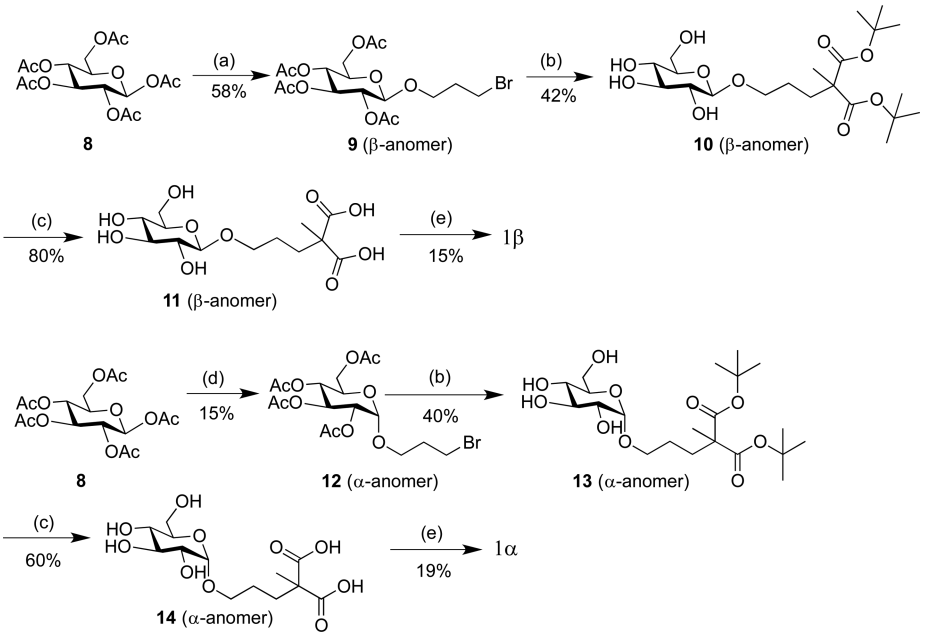

[a]Reagents and conditions: (a) 3-bromopropanol, BF_3-OEt_2, 20 h; b) (i) 2-methyl-di-*tert*-butyl malonate, NaH, DMF, 24 h; (ii) NaOMe, MeOH, 2 h; (c) TFA, DCM, 5 h; (d) (i) 3-bromopropanol, BF_3-OEt_2, 20 h, (ii) anhydrous $FeCl_3$, DCM, 36 h; (e) (i) $(DACH)PtCl_2$, Ag_2SO_4, H_2O, 20 h, (ii) $Ba(OH)_2$, H_2O, 24 h.[36,37]

RESULTS AND DISCUSSION

Synthesis of Positional Isomers. Glucose conjugates were designed in which attachment to the sugar moiety via a spacer preserved key structural features of the entity, a prerequisite for optimal glucose-transporter recognition. D-glucose offers five hydroxyl groups to which the spacer can be appended. Here we attached a biologically active platinum anticancer drug candidate **7** (Figure 2) to the different positions of D-glucose iteratively via a two carbon spacer using an ether glycosidic linkage.[27] The rigorous syntheses of the complete set of positional isomers with the same linker length of the glucose–platinum conjugates involve multiple steps, with several selective protection and deprotection steps.

The synthesis of the C1 derivatives is relatively facile and summarized in Scheme 1. The special reactivity profile offered by the anomeric "OAc" group of β-D-glucose penta-acetate (**8**) allows Lewis acid catalyzed regioselective introduction of 3-bromo-propanol at the C1 position. Both anomers of the desired C1-substituted glucose–malonic acid derivatives **11** and **14** could be synthesized from the starting material **8**. Treatment of **8** with 3-bromo-propanol in the presence of BF_3-OEt_2 provided compound **9** exclusively as the β-anomer. Formation of only a small amount (10–15%) of the α-anomer (**12**) was observed, which was removed during chromatographic purification. Compound **9** was then subjected to a nucleophilic substitution reaction with 2-methyl-di-*tert*-butyl malonate followed by deprotection of the acetyl-protecting groups using NaOMe. The resulting intermediate **10** was treated with trifluoroacetic acid (TFA) to obtain the desired glucose–malonic acid derivative **11**. For the synthesis of **14**, which is the α-anomer of **11**, $FeCl_3$-mediated anomerization was performed after installation of the 3-bromo-propanol unit at the C1 position of **8** in the first step.[38] The α-anomer **12** was isolated in 15% overall yield after two steps. Subsequently, a similar reaction sequence as that described for the synthesis of **11** yielded ligand **14**. The last synthetic step involved platination of ligands **11** or **14** with [dichloro(1*R*,2*R*)-cyclohexane-1,2-amine)platinum(II)], $[(DACH)PtCl_2]$,[39] which gave the C1-substituted Glc-Pts **1β** and **1α**, respectively. The anomeric purity of the C1-Glc-Pts was confirmed by their respective ^{1}H NMR spectra (Figure S6). The C1 anomeric proton signals of **1β** and **1α** appear at 4.45 ppm (d, J = 7.9 Hz) and 4.97 ppm (d, J = 3.7 Hz) in their respective NMR spectra. Furthermore, the coupling constants (J = 7.9 Hz for β and 3.7 Hz for α) confirmed the nature of the anomers of **1**.[40] As expected, significant differences in the ^{13}C NMR signals of **1β** and **1α** were also noticed. The C1 anomeric carbon resonances appeared at 102.3 and 98.2 ppm for **1β** and **1α**, respectively. These spectroscopic data confirm the distinct molecular configurations of **1β** and **1α**.

In contrast to the C1-Glc-Pts, the synthesis of C2-Glc-Pt **2** involves a 12-step route, which is presented in Scheme 2. The synthesis was initiated from commercially available, partially protected 1,2-*O*-isopropylidene-α-D-glucofuranose (**15**) followed by subsequent conversion to the fully protected derivative, **16**.[41] Efforts to synthesize intermediate **18**[42] from **16** in a one-step procedure using benzyl alcohol and either HCl or BF_3-OEt_2 were unsuccessful.[43] Although formation of **18** was traced by thin-layer chromatography (TLC) and electrospray ionization (ESI) mass spectrometry, the purification was tedious, requiring the removal of several undesired impurities present in the reaction mixture. Changing the ratio of reactants (benzyl alcohol and acid) and/or reaction conditions (temperature and/or time) also did not help. Finally, **18** was synthesized in two steps from **16** in good yield. Compound **18** was then subjected to nucleophilic substitution with allyl bromide in the presence of NaH to insert the alkyl chain at the C2 position. Hydroboration–oxidation of **19** afforded compound **20**. The hydroxyl group of **20** was then transformed into bromide **21** using an Appel reaction, and subsequent nucleophilic substitution with 2-methyl-di-*tert*-butyl malonate in the presence of NaH provided

DOI: 10.1021/jacs.6b06937
J. Am. Chem. Soc. 2016, 138, 12541–12551

Scheme 2. Synthesis of C2-Glc-Pt 2[a]

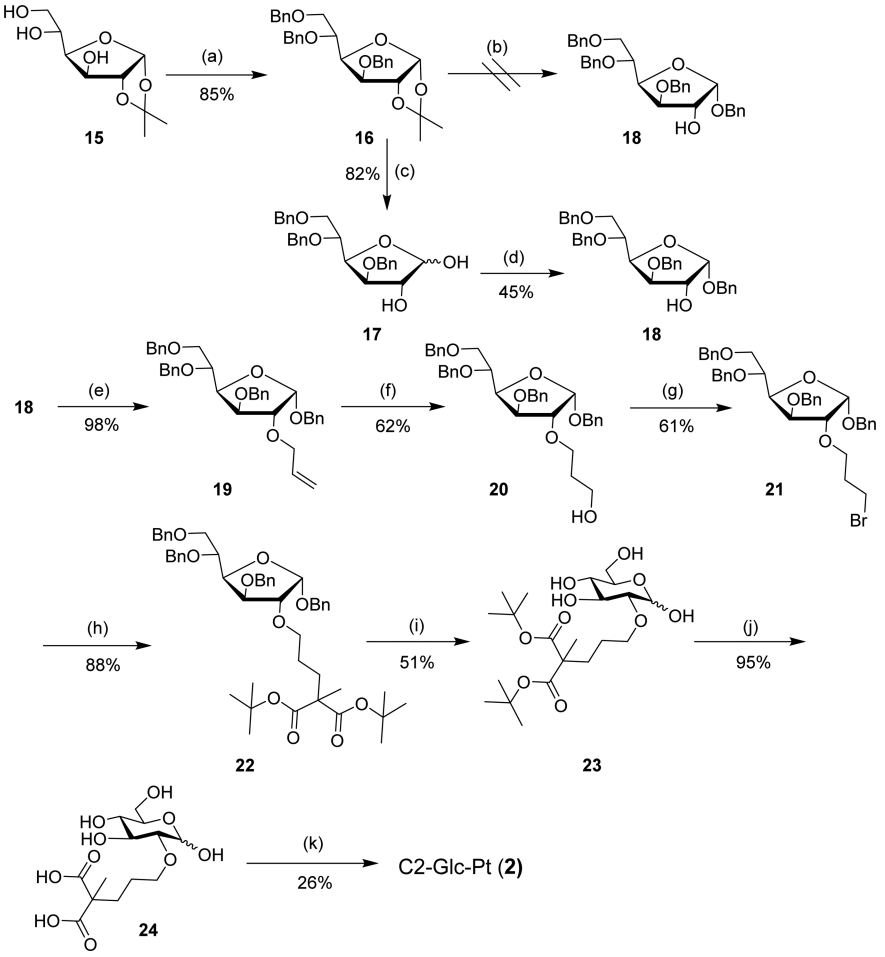

[a]Reagents and conditions: (a) BnBr, NaH, DMF; (b) BnOH, HCl in Et_2O or BF_3−OEt_2; (c) TFA, H_2O, DCM; (d) (i) di-butyl tin(IV) oxide, (ii) BnBr, K_2CO_3; (e) allyl bromide, NaH; (f) (i) $NaBH_4$, BF_3−OEt_2, (ii) NaOH, H_2O_2; (g) PPh_3, CBr_4; (h) 2-methyl-di-*tert*-butyl malonate, NaH, DMF; (i) Pd/C, H_2; (j) TFA, DCM; (k) (i) (DACH)$PtCl_2$, Ag_2SO_4, H_2O, 20 h, (ii) $Ba(OH)_2$, H_2O, 24 h.

Scheme 3. Synthesis of C3-Glc-Pt 3[a]

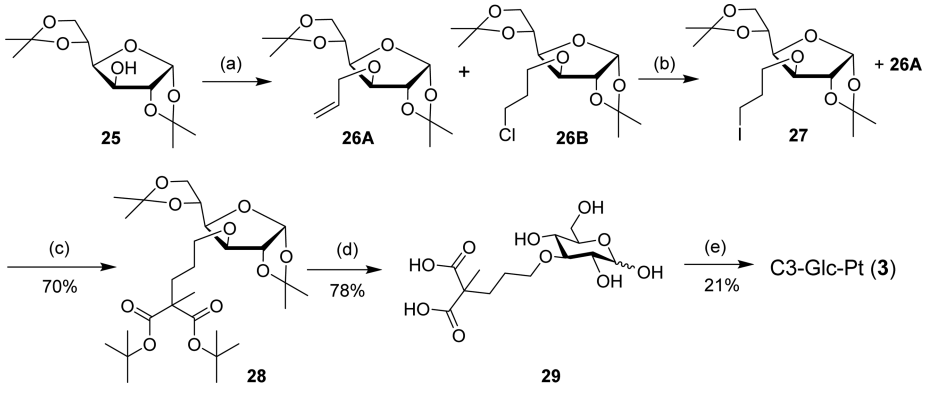

[a]Reagents and conditions: (a) 1-chloro-3-bromo-propane, 50% NaOH, DMSO; (b) NaI, acetone, reflux; (c) 2-methyl-di-*tert*-butyl malonate, NaH, DMF; (d) TFA, H_2O, DCM; (e) (i) (DACH)$PtCl_2$, Ag_2SO_4, H_2O, 20 h, (ii) $Ba(OH)_2$, H_2O, 24 h.

22. The protecting groups of **22** were removed in a two-step procedure to give the desired ligand **24**. Subsequently, C2-Glc-Pt **2** was prepared following a procedure similar to that described for the C1-Glc-Pts.

Commercial availability of the partially protected 1,2:5,6-di-*O*-isopropylidene-*α*-D-glucofuranose (**25**, Scheme 3), where all the hydroxyl groups, except that on C3, are protected, makes the synthesis of C3-Glc-Pt (**3**) plausible. As shown in Scheme 3, **25** was treated with 1-chloro-3-bromo-propane in the presence of NaOH to append the alkyl spacer to the C3 position of the sugar unit. The reaction yielded a 1:1 mixture of the desired **26B** and an undesired byproduct **26A**. The separation of **26B** from the

DOI: 10.1021/jacs.6b06937
J. Am. Chem. Soc. 2016, 138, 12541−12551

Scheme 4. Synthesis of C4-Glc-Pt 4[a]

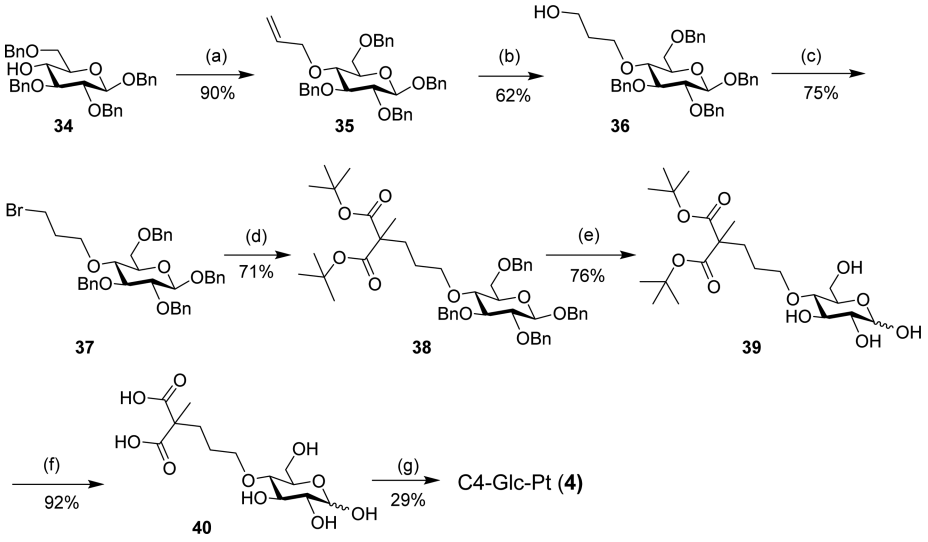

[a]Reagents and conditions: (a) allyl bromide, NaH; (b) (i) $NaBH_4$, $BF_3{-}OEt_2$, (ii) NaOH, H_2O_2; (c) PPh_3, CBr_4; (d) 2-methyl-di-*tert*-butyl malonate, NaH, DMF; (e) Pd/C, H_2; (f) TFA, DCM; (g) (i) (DACH)$PtCl_2$, Ag_2SO_4, H_2O, 20 h, (ii) $Ba(OH)_2$, H_2O, 24 h.

Table 1. IC_{50} Values for Glc-Pts 1−4, 6, and Aglycone 7 in DU145 Prostate Cancer (7.5 and 72 h Assays) and MRC5 Non-cancerous Lung Epithelial (72 h Assay) Cells

		IC_{50} values[a] (μM)						
cell line	incubation time (h)	**1β**	**1α**	**2**	**3**	**4**	**6**	**7**
DU145	7.5	12 ± 2	11 ± 1	9 ± 0.5	26 ± 4	18 ± 2	19 ± 1	10.4 ± 0.4
DU145	72	2.6 ± 0.08	3.7 ± 0.07	2.8 ± 0.27	3.4 ± 0.21	2.4 ± 0.14	2.4 ± 0.35	1.4 ± 0.51
MRC5	72	13 ± 6.2	>100	>100	93.6 ± 15	72.3 ± 5.8	95.5 ± 19	34.7 ± 8.8

[a]Data reflect the mean ± SD of results from three or more independent experiments, each performed in triplicate.

mixture was impossible because both **26A** and **26B** eluted together during chromatographic purification. We therefore used the mixture for subsequent steps. Treatment of the mixture with NaI followed by a nucleophilic substitution reaction with 2-methyl-di-*tert*-butyl malonate yielded **28**. The unreacted **26A** could be easily separated from the mixture in this step. Treatment of **28** with trifluoroacetic acid resulted in the required ligand **29**, which was then platinated to give the desired C3-Glc-Pt **3**.

For the synthesis of C4-Glc-Pt (**4**), we required a glucose derivative where all the hydroxyl groups, with exception of the C4 hydroxyl, were protected (**34** in Scheme 4). The synthetic route is depicted in Scheme 4. Similar to C1-Glc-Pts, synthesis of **4** was initiated from β-D-glucose penta-acetate (**8**) which was converted to **34** by a five-step procedure (Scheme S1).[44] The desired ligand **40** was then obtained using the exact same reaction sequence as used for the synthesis of **24** from **18** (Scheme 2). The last synthetic step involves platination of **40** to give **4**. The C6-Glc-Pt **6** and aglycone **7** were synthesized following recently reported synthetic routes.[27]

All new compounds were characterized by NMR (^1H, ^{13}C, ^{195}Pt) spectroscopy and ESI mass spectrometry. Purities of the platinum compounds were confirmed to be ≥95% by elemental microanalysis and analytical HPLC (see Supporting Information for details).

Cytotoxicity Profile of Glc-Pts 1−4 and 6. Having obtained all the positional isomers of Glc-Pt, we first investigated whether the position of substitution influences their anti-proliferation properties. The cytotoxicity was evaluated against a panel of cancer cell lines and a non-cancerous one by the MTT (3-(4,5-dimethylthiazol-2-yl)-2,5-diphenyltetrazolium bromide) assay. The potencies were expressed as IC_{50} values, which represent the concentration of the compounds that confer 50% growth inhibition. DU145 (prostate), A2780 (ovarian), A549 (lung) cancers, and MRC5 (non-cancerous lung fibroblast) cells were treated with Glc-Pts **1**−**4** and **6** for 72 h, after which the cell viabilities were evaluated. As shown in Table S1, all the Glc-Pts exhibit high potency and inhibited cancer cell growth at IC_{50} values of 0.07−0.32 μM (A2780), 1.7−4.2 μM (A549), and 2.4−3.7 μM (DU145). This tight distribution of IC_{50} values for the Glc-Pts against all the three cancer cell lines in the assay indicates that the position of substitution does not have a significant influence on cytotoxicity when cells were incubated for 72 h with the compounds. From our recent work on the C6-glucose−platinum conjugates we learned that the incubation time plays an important role in determining the cytotoxicity of this class of compounds.[27] We therefore treated DU145 cells with the compounds for 7.5 h instead of 72 h, followed by 64 h incubation in fresh media. As shown in Table 1, significant differences in the IC_{50} values among the Glc-Pts emerged under these conditions. Glucose conjugate **2** (IC_{50} = 9 μM) displayed approximately 3 times greater potency compared to **3** (IC_{50} = 26 μM), with the overall order of potency being **2** ≥ **1α** = **1β** ≥ **4** = **6** ≥ **3**. These results indicate that C1 and C2 substitution of D-glucose is preferred over that at C3, C4, and C6 for conveying cytotoxicity of the glycoconjugates in cancer cells.

As shown in Tables 1 and S1, in contrast to the cancerous cells, where low micromolar IC_{50} values were recorded for all Glc-Pts, several fold higher IC_{50} values were observed for non-cancerous

DOI: 10.1021/jacs.6b06937
J. Am. Chem. Soc. 2016, 138, 12541−12551

MRC5 lung fibroblast cells for all Glc-Pts in the 72 h MTT assay, the exception being **1β**. Notably, **1α** and **1β** are C1 positional isomers, but the IC_{50} value of **1α** is >100 μM whereas the same for **1β** is <20 μM in MRC5 cells (Table S1 and Figure S7a), suggesting that the configuration at the anomeric center has an important role in determining the cytotoxicity of glucose conjugates.

Whole-Cell Uptake Studies. In order to investigate whether the position of substitution has an influence on the cellular uptake of glucose conjugates, we studied the whole-cell uptake of Glc-Pts using DU145, A2780, SKOV3, and A549 cell lines. All express high levels of the GLUT1 transporter.[27,45] Cells were treated with compounds for 7.5 h, and the uptake of the Glc-Pts was determined by measuring the platinum content by atomic absorption spectroscopy.

It is expected that the distinctive structural and molecular conformations of the Glc-Pts under investigation will influence their function as substrates for glucose transporters. As shown in Figure 3, the cellular uptake of Glc-Pts may vary with the position

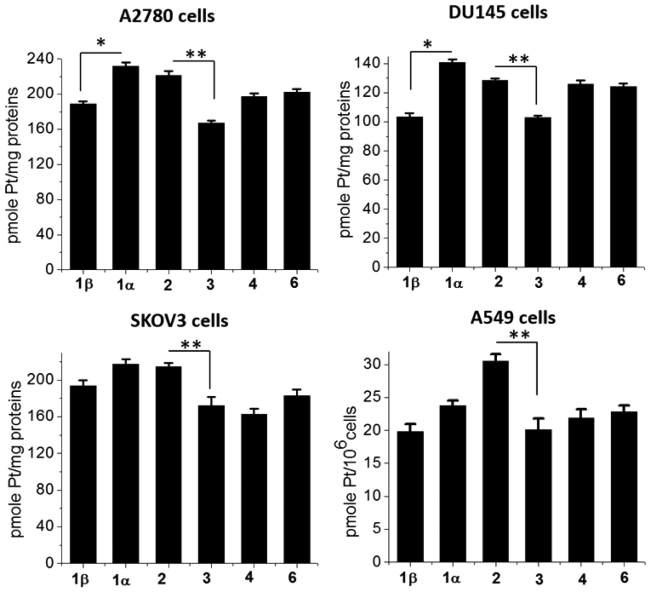

Figure 3. Whole-cell uptake of Glc-Pts **1**−**4** and **6** in DU145, A2780, SKOV3, and A549 cancer cells (compound concentration 20 μM for A2780, DU145, and SKOV3 cells and 40 μM for A549 cells; incubation time 7.5 h). Data represent the mean ± SD of at least three replicates. The asterisks denote differences that statistically significant (*$P < 0.01$, **$P < 0.001$).

of substitution. In addition, the extent of variation in uptake is also cell line dependent. Irrespective of the cancer cell type, the uptake of **2** is significantly higher than that of **3**. Strikingly, of the two anomers of **1**, uptake of **1α** is higher than that of **1β** in A2780 and DU145 cancer cells. These results are consistent with previously reported C1-substituted Cy3-glucose conjugates, where a relatively higher accumulation of the α-anomer was noticed compared to its β-anomer.[31] The preferential uptake of C-1 substituted α-anomer of a glycoconjugate in cancer cells is attributed to its relatively high recognition by facilitative glucose transporters.[2] In a recently published crystal structure of D-glucose bound to human GLUT3, which shares 66% sequence homology with human GLUT1, the occupancy of the α-anomer in the substrate binding site was dominant (69%) over that of the β-anomer, despite the relative prevalence of the β-anomer in aqueous solution.[2] In A549 cells, **2** was taken up most efficiently, and **3** and **1β** were taken up least efficiently. These results confirm that the cellular uptake of glucose conjugates in cancer cells is dependent on the position of substitution of D-glucose. From their structural similarities, Glc-Pts **1**−**4** are expected to have octanol−water partition coefficients similar to that of Glc-Pt **6** (log $P = -2.1$).[27] The highly hydrophilic nature of Glc-Pts indicates that their cellular internalization via passive diffusion through the cellular lipid membrane is unlikely. Therefore, differences in uptake between different positional isomers in cancer cells most likely arise from differential glucose-transporter-mediated cellular internalization efficiencies.

The cellular uptake of Glc-Pts **1α**, **2**, and **3** could be correlated with IC_{50} values obtained from MTT assays performed over a 7.5 but not 72 h incubation period. For example, as shown in Figure 3, despite significantly higher uptake of **1α** and **2** compared to that of **3** in A2780 or DU145 cells, all displayed similar cytotoxicity (Tables 1 and S1). Determination of cytotoxicity using a short incubation time (7.5 h with compounds followed by 64 h with fresh media) in DU145 cells revealed **1α** and **2** to be more cytotoxic than **3**. This observation parallels the observed differences in the cellular uptake of these compounds. However, despite being taken up less efficiently, **1β** had an IC_{50} value similar to those of **1α** and **2** in DU145 cells.

As discussed earlier, despite having similar activities in various cancer cells, **1α** and**1β** largely differ in their activities in MRC5 cells in a 72 h MTT assay (Table1). In order to obtain additional insight, cellular uptake studies of **1α** and **1β** in MRC5 cells were performed. As shown in Figure S7b, accumulation of the **1β** anomer was 43% greater than that of the **1α** anomer. This difference in uptake at least in part explains the differential cytotoxicity profile of the two anomers of **1**. The results indicate that both the position of substitution and the anomeric configuration influence the biological properties of a glucose conjugate.

Cellular Uptake in Cancer Cells versus Matched Normal Cells. We next investigated whether the ability of Glc-Pts to accumulate selectively in cancer cells varies with the position of D-glucose substitution. The cellular uptake in prostate epithelial RWPE2 cells was investigated and compared with uptake in the matched prostate cancer DU145 cell line. Cancer cells, but not the normal healthy cells, upregulate the expression of glucose transporters and, consequently, glucose influx and utilization.[11−13] We recently showed that DU145 has an elevated level of GLUT1 expression, whereas the expression of GLUT1 was not even detectable for RWPE2 cells under a similar experimental condition.[27] Therefore, glycoconjugates capable of exploiting the membrane-associated glucose transporters are expected to accumulate in the DU145 cancer cells preferentially. Moreover, the position of substitution can modulate the uptake in DU145 but not RWPE2 cells. As shown in Figure S8a,b, the accumulation of all the Glc-Pts in DU145 cells is 3.7−5.5-fold higher than in RWPE cells. Importantly, as shown in Figure S8b, accumulation of all the Glc-Pts is similar in RWPE2 cells (25−30 pmol/mg proteins). However, statistically significant variations between different Glc-Pts in DU145 cells suggest that the position of substitution of D-glucose at the platinum warhead potentiates uptake in DU145 cells. The cellular uptake data together with differences in the level of glucose-transporter expression in DU145 and RWPE2 cells indicate that the variable accumulation of Glc-Pts arises, at least partly, from differential glucose-transporter-mediated translocation efficiencies of Glc-Pts.

DOI: 10.1021/jacs.6b06937
J. Am. Chem. Soc. 2016, 138, 12541−12551

Dependence of GLUT1 Specificity on Position of Substitution. The specific cancer-targeting ability of a glycoconjugate depends on how well it is recognized by or translocated through glucose transporters overexpressed in cancer cells. We therefore investigated how the position of substitution in D-glucose affects specific uptake of the resulting glycoconjugates. As discussed above, comparison of cellular uptake data in cancerous vs non-cancerous cells has already implicated glucose transporters in the uptake of Glc-Pts. Among the facilitative glucose transporters overexpressed in cancers, GLUT1 is the most common and best studied. It is broadly overexpressed in many different cancers, and its expression level in biopsy samples from cancer patients strongly correlates with tumor development, progression, and poor prognosis.[4−6] Here we screened the Glc-Pts for their ability to translocate specifically through GLUT1. Subsequently, the cellular uptake of the Glc-Pts was determined in the absence and in the presence of a specific GLUT1 inhibitor, cytochalasin B, in DU145 cells. The results are presented in Figure 4. As expected, uptake of aglycone **7** was not

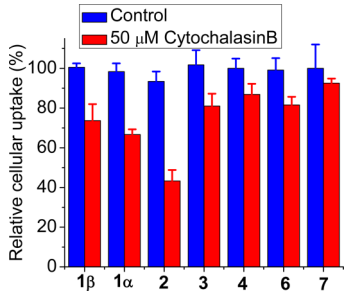

Figure 4. Effect of GLUT1 inhibitor cytochasinB on the cellular uptake of Glc-Pts **1**−**4**, **6**, and aglycone **7** in DU145 cells (compound concentration 80 μM, exposure time 2 h).

inhibited significantly, but different degrees of uptake inhibition were observed for the Glc-Pts. This result confirms our hypothesis that the position of substitution is an important parameter in determining the GLUT1 specificity of glycoconjugates. Cellular uptake of C2-Glc-Pt **2** was most significantly inhibited, by 57%, indicating substitution at C2 to be highly favorable for GLUT1 specificity of this class of glycoconjugates. The order of uptake inhibition by the GLUT1 inhibitor, which parallels the degree of GLUT1-specific uptake, is **2** > **1α** ≥ **1β** > **3** = **4** = **6**. We recently reported the synthesis and glucose-transporter-mediated uptake of C6-glucose platinum conjugates including **6**. The compounds were designed on the basis of the D-glucose-bound crystal structure of XylE, a bacterial GLUT homologue. Importantly, the current study confirms that the GLUT1 specificity of **2** is superior to **6**. However, we note that, together with GLUT1, different glucose-transporter isoforms such as GLUT2, GLUT3, GLUT4, SGLT1, and SGLT2 are expressed in tumors and cancer cells.[4] Owing to structural and functional variations, the order of specificity of Glc-Pts may not be the same for all glucose transporters. Moreover, owing to the presence of (1*R*,2*R*)-cyclohexane-1,2-diamine (DACH) as part of their structures, solute transporters such as organic cation transporter 2 (OCT2), other than GLUTs might, also contribute to the cellular uptake of these class of compounds.[27] In addition to glucose transporters, various enzymes such as hexokinase II and cell-proliferation-associated antigen Ki-67 play important roles in intracellular processing of D-glucose or glucose conjugates, thereby contributing indirectly to the cellular accumulation in cancer cells.[46−48] After gaining entry to the cells, ^{18}F-FDG is metabolized to ^{18}F-FDG-6-phosphate by hexokinase II that is overexpressed in cancers and effectively trapped inside the cells. Positive correlations between ^{18}F-FDG uptake and hexokinase II expression and activity in certain type of cancers and cancer cells have been reported.[47−49] β-Glucosidases comprise another class of enzymes that play important roles, especially in the activation of glycoconjugated prodrugs.[50,51] Recently, glycosylated Pt(IV) complexes bearing different glucuronic acids and linkers were synthesized to study antitumor activity. Despite having good *in vitro* activity owing to improved uptake when compared to their Pt(II) counterparts, the complexes did not show specific uptake by GLUTs.[52] The use of protected glucuronic acids explains the lack of GLUT-mediated uptake. Our glycoconjugation chemical approach circumvents this problem because we provide evidence for GLUT1 specificity based on the position of substitution on glucose.

In order to further ascertain whether the position of substitution is an important determinant of GLUT1 specificity of glycoconjugates, we determined and compared the cytotoxicity of Glc-Pts in DU145 and its GLUT1 knockdown clone (hereafter designated DU145-hGLUT1-shRNA). As shown in Figure 5a, approximately 50% knockdown of GLUT1 transporter

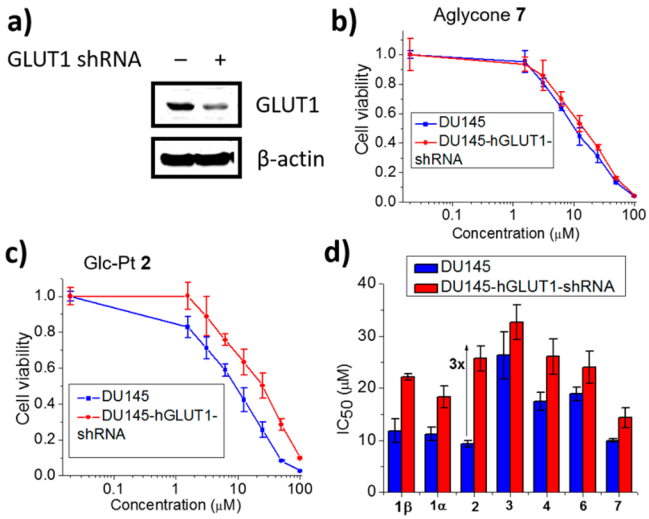

Figure 5. (a) Western blot analysis of GLUT1 protein in DU145 and its knockdown clone. (b,c) Representative dose−response curves for DU145 and DU145-hGLUT1-shRNA cells treated with different concentrations of the aglycone **7** and Glc-Pt **2**. Cells were treated with compounds for 7.5 h followed by incubation in fresh media for 64 h before the viability was evaluated by the MTT assay. (d) Comparison of IC_{50} values of Glc-Pts **1**−**4**, **6**, and **7** in DU145 and DU145-hGLUT1-shRNA cells.

expression was achieved by transfecting DU145 cells with a GLUT1-shRNA (see Experimental Section for details). The anticancer activity determined by MTT assays in DU145 and DU145-hGLUT1-shRNA cells revealed that the observed differences in cytotoxicity of Glc-Pts between wild type and GLUT1 knockdown cells are highly dependent on the position of substitution of D-glucose (Figure 5d). As expected, no significant differences in IC_{50} values of aglycone **7** were observed for DU145 and its GLUT1 knockdown clone (Figure 5b,d). However, the IC_{50} value of Glc-Pt **2** in DU145-hGLUT1-shRNA was determined to be 26 μM, which is 2.9-fold higher than the IC_{50}

DOI: 10.1021/jacs.6b06937
J. Am. Chem. Soc. 2016, 138, 12541−12551

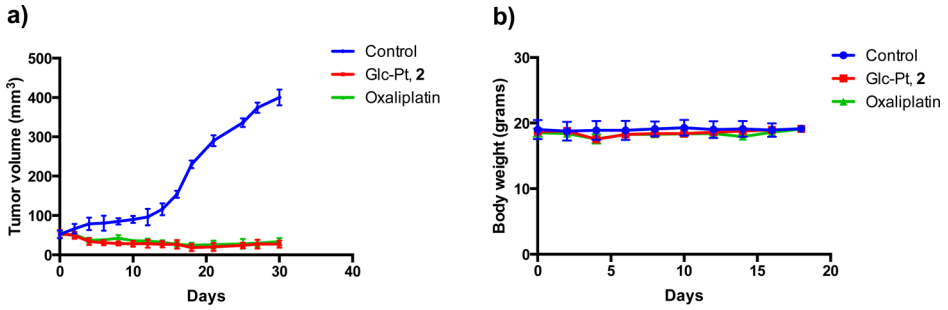

Figure 6. Treatment of GLUT1 breast cancer in a Balb/c syngeneic mouse model. Treatment began when tumors reached ~50 mm^3 and was given by an intravenous bolus injection of 5.0 mg/kg of oxaliplatin, Glc-Pt **2**, or PBS. Tumor volumes were monitored daily, and their total volume was normalized to initial tumor size at time of treatment. Each treatment group consisted of 5 animals (n = 5). (a) Antitumor efficacy studies. (b) Toxicity analysis by monitoring body weight after candidate drug administration.

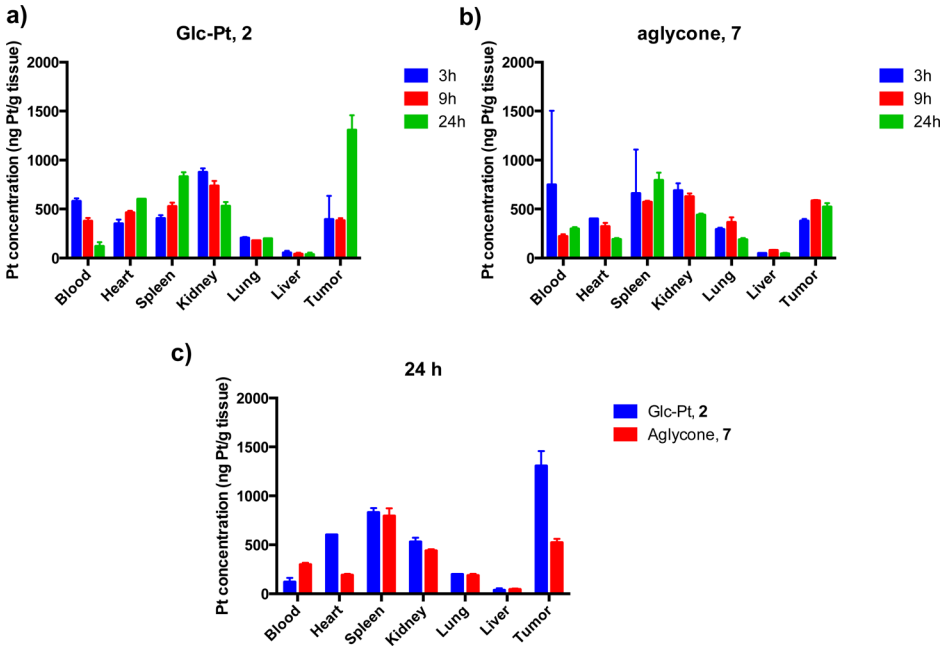

Figure 7. Biodistribution of Glc-Pt **2** or aglycone **7** in GLUT1 breast cancer tumor bearing animals. (a) Quantification of platinum concentration in organ tissue as measured by atomic absorption spectroscopy 3, 9, and 24 h following administration of Glc-Pt **2** after nitric acid digestion. (b) Quantification of platinum concentration in organ tissue as measured by atomic absorption spectroscopy 3, 9, and 24 h following administration of aglycone **7** after nitric acid digestion. (c) Comparative plot of platinum concentration in organ tissue of **2** and **7** at 24 h.

value for parental DU145 cells (9 μM) (Figure 5c,d). The potencies of the **1*β*** and **1*α*** decreased by 1.8- and 1.6-fold, respectively, upon knockdown of GLUT1 transporters, but there was no effect on the efficacy of **3**, **4**, and **6**. These results confirm that the highest GLUT1 specificity is displayed by C2-substituted Glc-Pt **2**, which is consistent with the highest cellular uptake inhibition of **2** by cytochalasin B.

***In Vivo* Efficacy and Biodistribution of Glc-Pt 2.** The *in vivo* anticancer activity of our best GLUT1-targeting molecule, Glc-Pt **2**, was assessed *in vivo* using a mouse model of GLUT1 expressing breast cancer (G1fpt),[53] a syngeneic model induced in Balb/c mice. Intravenous bolus injections of 5 mg/kg of Glc-Pt **2** or oxaliplatin commenced when tumors reached ~50 mm^3 for four successive treatments, once every other day. Treatment groups included Glc-Pt **2**, oxaliplatin, and a control group receiving PBS. Platinum complexes were freshly prepared by dissolution in PBS prior to injection. Antitumor efficacy was evaluated by measuring the tumor volume over a period of 30 days. Toxic side effects of the platinum agents under investigation were assessed daily by thorough examination of physical condition including body weight, lethargy, loss of appetite, and general behavior of the animals. The tumor treatment revealed that Glc-Pt **2** effectively reduces disease burden by significantly delaying tumor growth at a dose of 5 mg/kg (Figure 6a). Moreover, oxaliplatin treatment showed no statistically significant difference compared to the Glc-Pt **2** treated group. Notably, tumors treated with Glc-Pt, **2**, or oxaliplatin were 10 times smaller compared to tumors in the PBS-treated control group, indicating excellent efficacy.

The potential toxicity of the platinum constructs **2** and oxaliplatin, compared to PBS-treated controls, was assessed by monitoring the body weight and general behavior of the animals. Balb/c mice were treated with PBS, **2**, or oxaliplatin at the same dosing schedule used for the efficacy studies (5 mg/kg, four times in 8 days). As shown in Figure 6b, the body weight of mice treated with **2** or oxaliplatin was reduced after the second dose but recovered to normal values throughout the rest of the study, without further weight changes. Conceivably, despite minor changes in body weight, a more detailed toxicology study would more fully characterize the effects of **2**. Also, **2** or **7** accumulated

DOI: 10.1021/jacs.6b06937
J. Am. Chem. Soc. 2016, 138, 12541−12551

in the kidney and spleen but minimally in the liver at similar concentrations after 24 h, indicative of clearance. Renal filtration appears to be a major clearance pathway, which might be expected considering the hydrophilic nature of **2** and **7**.

The biodistribution of Glc-Pt **2** was assessed by graphite furnace atomic absorption spectroscopy (GFAAS) at 3, 9, and 24 h following administration (i.v.) in a mouse model bearing murine breast cancer overexpressing GLUT1; the results are shown in Figure 7. Given that Glc-Pt **2** displays selective GLUT1-mediated uptake *in vitro*, we were interested to learn whether this phenomenon persists *in vivo*. To investigate the GLUT1-mediated uptake of **2**, we used compound **7**, a non-targeted platinum complex, as control. It became evident after 24 h (Figure 7c) that **2** accumulates in tumor tissue approximately 3-fold better than **7**, which lacks a D-glucose-targeting ligand. This result is consistent with the *in vitro* uptake studies described above. The encouraging selectivity has the potential to overcome toxic side effects associated with platinum anticancer agents and subsequently to improve drug efficacy with the possibility of increasing drug dose without limiting toxicities. Overall, the biodistribution result confirms the anticancer efficacy of **2**, as demonstrated by selective targeting to tumor.

SUMMARY AND CONCLUSION

Feasible synthetic routes were established to all the positional isomers of Glc-Pt conjugates by means of ether−glycosidic linkages. To our knowledge, this is the first time that a platinum drug candidate has been attached via a spacer to each of the individual oxygen atoms of D-glucose. The synthetic strategies presented here provide a potential platform for the synthesis of any desired positional isomer of a glucose conjugate. The current investigation experimentally establishes that the position of substitution of D-glucose is an important parameter for the biological activity profile of the resulting glucose conjugate. Glc-Pts **1*α*** and **2** accumulate most efficiently in cancer cells compared to the other positional isomers. No significant differences in uptake of Glc-Pts were observed in non-cancerous cells that do not express GLUT1 transporter, suggesting that differential uptake in cancer cells arises mainly from the differential glucose-transporter-mediated uptake of the Glc-Pts. Furthermore, the site of substitution modulates the cytotoxicity profile of the Glc-Pts, with the C2-Glc-Pt **2** being most potent and C3-Glc-Pt **3** being the least potent of the positional isomers in DU145 cells. Cellular uptake studies in the absence and in the presence of the GLUT1 inhibitor cytochalasin B revealed that Glc-Pt **2** has the highest GLUT1-specific internalization ability. The GLUT1 specificity of **2** was further confirmed by comparing the potencies of all Glc-Pts in DU145 cells and in its GLUT1 knockdown clone. The results of this investigation again point to C2 as the most preferable position on D-glucose for attaching a warhead for GLUT1-mediated delivery of an anticancer agent. Additional experimental data on other C2-glucose conjugates are desired to confirm this initial observation. Compound **2** has antitumor efficacy in mice, comparable to that of oxaliplatin. Importantly, tumor uptake of **2** is significantly higher than that of its non-targeted analogue **7** *in vivo*. Although at this stage we do not know the specificity of Glc-Pts for other glucose-transporter isoforms, such as GLUT2−GLUT4, SGLT1, and SGLT2, our findings identify the position of substitution on D-glucose as an important descriptor of glucose-transporter specificity and biological activity of glycoconjugates *in vitro* and *in vivo*.

EXPERIMENTAL SECTION

General Procedure for the Synthesis of Glc-Pts. A suspension of dichlorido[(1*R*,2*R*)-cyclohexane-1,2-diamine]platinum(II)[39] ([DACH]$PtCl_2$) and Ag_2SO_4 in water was stirred overnight at room temperature in the dark. The precipitate was filtered off using a 0.2 μm syringe filter, and the filtrate containing [DACH]$PtSO_4$ was added in a dropwise manner to an aqueous solution of the corresponding ligand and $Ba(OH)_2{\cdot}8H_2O$ in water, which had been initially stirred for 30 min at room temperature. The reaction mixture was then stirred for 20 h in the dark before removal of insoluble $BaSO_4$ by filtration. The filtrate was lyophilized, and the milky white solid obtained was purified using preparative HPLC with a linear gradient of Millipore water (A) and methanol (B; Sigma-Aldrich HPLC-grade): t = 0−5 min, 15% B; t = 8 min, 13% B; t = 30 min, 55% B; t = 35 min, 95% B. The flow rate was 15 mL min^{-1}, and UV absorption was measured at 220 nm.

Animal Facility and Standard of Care. Mice were placed in a facility accredited by the Institutional Animal Care and Use Committee. Treatments were administered by retro-orbital injection of the venous sinus. Amount of anticancer agents was calculated on the basis of the average animal body weight. The MIT Committee for Animal Care approved all animal protocols.

Glc-Pt 1*β*. Reagents used: [DACH]$PtCl_2$ (123 mg, 0.32 mmol) and Ag_2SO_4 (99 mg, 0.32 mmol) in water (3 mL); **11** (110 mg, 0.32 mmol) and $Ba(OH)_2{\cdot}8H_2O$ (103 mg, 0.32 mmol) in water (4 mL). Glc-Pt **1*β*** was obtained as a white powder (yield: 31 mg, 15%). t_R (RP-HPLC) = 13.1 min. ^{1}H NMR (400 MHz, D_2O): δ (ppm) 0.99−1.08 (m, 2H, CH_2 DACH),1.13−1.29 (m, 5H, CH_2 DACH and CH_3), 1.42−1.66 (m, 4H, CH_2 DACH and OCH$_2$CH_2CH$_2$), 1.89−2.01 (m, 2H, CH_2 DACH), 2.26−2.36 (m, 2H, 2 × CH DACH), 2.75−2.97 (m, 2H, OCH$_2$CH$_2$CH_2), 3.15−3.46 (m, 4H, OCH_2CH$_2$CH$_2$, and 2 × CH), 3.58−4.01 (m, 4H, OHCH_2 and 2 × CH) 4.45 (d, J = 7.9 Hz, 1H, CH anomeric). ^{13}C{^{1}H} NMR (100 MHz, D_2O): δ (ppm) 181.76, 181.66, 102.21, 75.92, 75.79, 73.23, 70.22, 69.66, 62.51, 62.27, 60.71, 56.90, 35.76, 31.79, 31.69, 24.88, 23.85, 20.85. ^{195}Pt{^{1}H} NMR (86 MHz, D_2O): δ (ppm) −1891. ESI-MS (pos. detection mode): m/z (%): 668.3 (100) $[M+Na]^+$, calculated m/z for $[M+Na]^+$ 668.2. Anal. Calcd for $C_{19}H_{34}N_2O_{10}Pt{\cdot}(H_2O)_2$: C, 33.48; H, 5.62; N, 4.11. Found: C, 33.07; H, 5.15; N, 3.99.

Glc-Pt 1*α*. Reagents used: [DACH]$PtCl_2$ (137 mg, 0.35 mmol) and Ag_2SO_4 (110 mg, 0.35 mmol) in water (4 mL); **14** (120 mg, 0.35 mmol) and $Ba(OH)_2{\cdot}8H_2O$ (114 mg, 0.35 mmol) in water (4 mL). Glc-Pt **1*α*** was isolated as a white powder (yield: 45 mg, 19%). t_R (RP-HPLC) = 13.3 min. ^{1}H NMR (400 MHz, D_2O): δ (ppm) 0.97−1.08 (m, 2H, CH_2 DACH),1.13−1.31 (m, 5H, CH_2 DACH and CH_3), 1.42−1.64 (m, 4H, CH_2 DACH and OCH$_2$CH_2CH$_2$), 1.90−1.99 (m, 2H, CH_2 DACH), 2.30−2.38 (m, 2H, 2 × CH DACH), 2.60−2.67 (m, 1H, OCH$_2$CH$_2$CH_2), 3.10−3.11 (m, 1H, OCH$_2$CH$_2$CH_2), 3.33−3.37 (m, 1H, OCH_2CH$_2$CH$_2$), 3.47−3.52 (m, 1H, OCH_2CH$_2$CH$_2$), 3.57−3.79 (m, 6H, HOCH_2 and 4 × CH), 4.97 (d, J = 3.7 Hz, 1H, CH anomeric). ^{13}C{^{1}H} NMR (100 MHz, D_2O): δ (ppm) 181.87, 181.61, 98.12, 73.14, 71.98, 71.33, 69.55, 67.90, 62.43, 62.35, 60.55, 56.93, 36.28, 31.81, 31.62, 24.82, 23.83, 20.65. ^{195}Pt{^{1}H} NMR (86 MHz, D_2O): δ (ppm) −1886. ESI-MS (pos. detection mode): m/z (%) 646.2 (100) $[M+H]^+$, calculated m/z for $[M+H]^+$ 646.5. Anal. Calcd for $C_{19}H_{34}N_2O_{10}Pt{\cdot}2(H_2O)$: C, 33.48; H, 5.62; N, 4.11. Found: C, 33.37; H, 5.31; N, 4.41.

Glc-Pt 2. Reagents used: [DACH]$PtCl_2$ (171 mg, 0.45 mmol) and Ag_2SO_4 (137 mg, 0.45 mmol) in water (6 mL); **24** (152 mg, 0.45 mmol) and $Ba(OH)_2{\cdot}8H_2O$ (141 mg, 0.45 mmol) in water (5 mL). Glc-Pt **2** was isolated as a white powder (yield: 75 mg, 26%). t_R (RP-HPLC) = 12.5 and 13.0 min (α and β anomers). ^{1}H NMR (400 MHz, D_2O): δ (ppm) 1.03−1.13 (m, 2H, CH_2 DACH), 1.14−1.29 (m, 5H, CH_2 DACH and CH_3), 1.46−1.62 (m, 4H, 2 × CH_2 DACH), 1.94−2.01 (m, 2H, OCH$_2$CH_2CH$_2$), 2.28−2.37 (m, 2H, 2 × CH DACH), 2.72−3.01 (m, 2H, OCH$_2$CH$_2$CH_2), 3.27−3.49 (m, 3H, OCH_2CH$_2$CH$_2$ and CH), 3.71−3.81 (m, 5H, HOCH_2 and 3 × CH), 4.62 (d, J = 7.9 Hz, 0.5H, CH anomeric), 5.39 (d, J = 3.4 Hz, 0.5H, CH anomeric). ^{13}C{^{1}H} NMR (100 MHz, D_2O): δ (ppm) 181.69, 181.56, 126.66, 95.88, 90.11, 82.71, 79.44, 75.84, 75.44, 73.03, 72.19, 71.20, 70.66, 69.75, 69.66, 62.83, 62.73, 62.58, 62.47, 62.31, 60.69, 60.54, 57.03, 57.02, 35.98, 35.89, 31.96, 31.79,

DOI: 10.1021/jacs.6b06937
J. Am. Chem. Soc. 2016, 138, 12541−12551

25.36, 25.24, 23.93, 23.88, 20.83, 20.75. ^{195}Pt{^{1}H} NMR (86 MHz, D_2O): δ (ppm) −1876. ESI-MS (pos. detection mode): m/z (%) 646.2 (100) $[M+H]^+$, calculated m/z for $[M+H]^+$ 646.5. Anal. Calcd for $C_{19}H_{34}N_2O_{10}Pt\cdot(H_2O)_2\cdot2(CF_3COOH)$: C, 30.37; H, 4.43; N, 3.08. Found: C, 30.55; H, 4.24; N, 3.37. ^{19}F{^{1}H} NMR (376 MHz, D_2O): δ (ppm) −75.6 (residual trifluoroacetic acid).

Glc-Pt 3. Reagents used: [DACH]$PtCl_2$ (137 mg, 0.35 mmol) and Ag_2SO_4 (110 mg, 0.35 mmol) in water (4 mL); **29** (120 mg, 0.35 mmol) and $Ba(OH)_2\cdot8H_2O$ (114 mg, 0.35 mmol) in water (4 mL). Glc-Pt **3** was isolated as a white powder (yield: 48 mg, 21%). t_R (RP-HPLC) = 13.0 and 13.3 min (α and β anomers). ^{1}H NMR (400 MHz, D_2O): δ (ppm) 0.96−1.11 (m, 2H, CH_2 DACH), 1.12−1.30 (m, 5H, CH_2 DACH and CH_3), 1.42−1.64 (m, 4H, 2 × CH_2 DACH), 1.88−2.02 (m, 2H, $OCH_2CH_2CH_2$), 2.25−2.37 (m, 2H, 2 × CH DACH), 2.74−3.05 (m, 2H, $OCH_2CH_2CH_2$), 3.16−3.45 (m, 3H, $OCH_2CH_2CH_2$ and CH), 3.48−3.92 (m, 5H, $HOCH_2$ and 3 × CH), 4.57 (d, J = 7.8 Hz, 0.6H, CH anomeric), 5.13 (d, J = 6.5 Hz, 0.4H, CH anomeric). ^{13}C{^{1}H} NMR (100 MHz, D_2O): δ (ppm) 181.80, 181.66, 95.92, 92.17, 84.46, 81.74, 75.89, 73.90, 73.26, 73.10, 71.56, 71.32, 69.26, 69.22, 62.56, 62.27, 60.63, 60.46, 56.97, 36.02, 31.81, 31.70, 25.43, 23.88, 23.84, 20.73. ^{195}Pt{^{1}H} NMR (86 MHz, D_2O): δ (ppm) −1888. ESI-MS (pos. detection mode): m/z (%) 646.2 (100) $[M+H]^+$, calculated m/z for $[M+H]^+$ 646.5. Anal. Calcd for $C_{19}H_{34}N_2O_{10}Pt\cdot(H_2O)_3$: C, 32.62; H, 5.76; N, 4.00. Found: C, 32.71; H, 5.73; N, 4.01.

Glc-Pt 4. Reagents used: [DACH]$PtCl_2$ (171 mg, 0.45 mmol) and Ag_2SO_4 (137 mg, 0.45 mmol) in water (6 mL); **40** (152 mg, 0.45 mmol) and $Ba(OH)_2\cdot8H_2O$ (141 mg, 0.45 mmol) in water (5 mL). Glc-Pt **4** was isolated as a white powder (yield: 85 mg, 29%). t_R (RP-HPLC) = 12.6 and 12.7 min (α and β anomers). ^{1}H NMR (400 MHz, D_2O): δ (ppm) 1.01−1.14 (m, 2H, CH_2 DACH), 1.17−1.29 (m, 5H, CH_2 DACH and CH_3), 1.45−1.58 (m, 4H, 2 × CH_2 DACH), 1.92−2.02 (m, 2H, $OCH_2CH_2CH_2$), 2.25−2.37 (m, 2H, 2 × CH DACH), 2.77−2.98 (m, 2H, $OCH_2CH_2CH_2$), 3.16−3.31 (m, 2H, $OCH_2CH_2CH_2$), 3.39−3.56 (m, 2H, 2 × CH), 3.68−3.95 (m, 4H, $HOCH_2$ and 2 × CH), 4.55 (d, J = 8 Hz, 0.6H, CH anomeric), 5.13 (d, J = 7.2 Hz, 0.4H, CH anomeric). ^{13}C{^{1}H} NMR (100 MHz, D_2O): δ (ppm) 181.66, 181.61, 95.87, 91.96, 78.28, 78.20, 75.67, 75.12, 74.25, 73.13, 72.72, 71.59, 70.59, 62.72, 62.61, 62.26, 60.60, 60.51, 56.95, 36.11, 36.01, 31.85, 31.71, 25.38, 23.91, 20.75. ^{195}Pt{^{1}H} NMR (86 MHz, D_2O): δ (ppm) −1883. ESI-MS (pos. detection mode): m/z (%) 646.2 (100) $[M+H]^+$, calculated m/z for $[M+H]^+$ 646.5. Anal. Calcd for $C_{19}H_{34}N_2O_{10}Pt\cdot(CF_3COOH)_3$: C, 30.40; H, 3.78; N, 2.84. Found: C, 30.12; H, 3.45; N, 3.30.

Glc-Pt 6. Glc-Pt **6** was prepared following a literature procedure.[27]

■ ASSOCIATED CONTENT

Supporting Information

The Supporting Information is available free of charge on the ACS Publications website at DOI: 10.1021/jacs.6b06937.

Materials and methods, experimental details, characterization data, NMR spectra of compounds, analytical HPLC traces of Glc-Pts, and cellular and animal studies, including Scheme S1, Table S1, and Figures S1−S8 (PDF)

■ AUTHOR INFORMATION

Corresponding Author

*lippard@mit.edu

Notes

The authors declare no competing financial interest.

■ ACKNOWLEDGMENTS

This work was supported by NCI Grant CA034992.

■ REFERENCES

(1) Calvo, M. B.; Figueroa, A.; Pulido, E. G.; Campelo, R. G.; Aparicio, L. A. *Int. J. Endocrinol.* **2010**, *2010*, 205357.

(2) Deng, D.; Sun, P.; Yan, C.; Ke, M.; Jiang, X.; Xiong, L.; Ren, W.; Hirata, K.; Yamamoto, M.; Fan, S.; Yan, N. *Nature* **2015**, *526*, 391.

(3) Deng, D.; Xu, C.; Sun, P.; Wu, J.; Yan, C.; Hu, M.; Yan, N. *Nature* **2014**, *510*, 121.

(4) Szablewski, L. *Biochim. Biophys. Acta, Rev. Cancer* **2013**, *1835*, 164.

(5) Ohba, S.; Fujii, H.; Ito, S.; Fujimaki, M.; Matsumoto, F.; Furukawa, M.; Yokoyama, J.; Kusunoki, T.; Ikeda, K.; Hino, O. *J. Oral Pathol. Med.* **2010**, *39*, 74.

(6) Kunkel, M.; Moergel, M.; Stockinger, M.; Jeong, J.-H.; Fritz, G.; Lehr, H.-A.; Whiteside, T. L. *Oral Oncol.* **2007**, *43*, 796.

(7) Guo, G. F.; Cai, Y. C.; Zhang, B.; Xu, R. H.; Qiu, H. J.; Xia, L. P.; Jiang, W. Q.; Hu, P. L.; Chen, X. X.; Zhou, F. F.; Wang, F. *Med. Oncol.* **2011**, *28*, 197.

(8) Ishikawa, N.; Oguri, T.; Isobe, T.; Fujitaka, K.; Kohno, N. *Jpn. J. Cancer Res.* **2001**, *92*, 874.

(9) Vander Heiden, M. G.; Cantley, L. C.; Thompson, C. B. *Science* **2009**, *324*, 1029.

(10) Warburg, O. *Science* **1956**, *123*, 309.

(11) Cantor, J. R.; Sabatini, D. M. *Cancer Discovery* **2012**, *2*, 881.

(12) Bronstein, Y.; Tummala, S.; Rohren, E. *Clin. Nucl. Med.* **2011**, *36*, 96.

(13) Vander Heiden, M. G. *Nat. Rev. Drug Discovery* **2011**, *10*, 671.

(14) Calvaresi, E. C.; Hergenrother, P. J. *Chem. Sci.* **2013**, *4*, 2319.

(15) Kim, W. H.; Lee, J.; Jung, D.-W.; Williams, D. R. *Sensors* **2012**, *12*, 5005.

(16) Som, P.; Atkins, H. L.; Bandoypadhyay, D.; Fowler, J. S.; MacGregor, R. R.; Matsui, K.; Oster, Z. H.; Sacker, D. F.; Shiue, C. Y.; Turner, H.; Wan, C.-N.; Wolf, A. P.; Zabinski, S. V. *J. Nucl. Med.* **1980**, *21*, 670.

(17) Bowen, M. L.; Orvig, C. *Chem. Commun.* **2008**, 5077.

(18) Schibli, R.; Dumas, C.; Petrig, J.; Spadola, L.; Scapozza, L.; Garcia-Garayoa, E.; Schubiger, P. A. *Bioconjugate Chem.* **2005**, *16*, 105.

(19) Welling, M. M.; Alberto, R. *Nucl. Med. Commun.* **2010**, *31*, 239.

(20) Storr, T.; Obata, M.; Fisher, C. L.; Bayly, S. R.; Green, D. E.; Brudzinska, I.; Mikata, Y.; Patrick, B. O.; Adam, M. J.; Yano, S.; Orvig, C. *Chem. - Eur. J.* **2005**, *11*, 195.

(21) Ben-Haim, S.; Ell, P. *J. Nucl. Med.* **2009**, *50*, 88.

(22) Chen, Y.; Heeg, M. J.; Braunschweiger, P. G.; Xie, W.; Wang, P. G. *Angew. Chem., Int. Ed.* **1999**, *38*, 1768.

(23) Liu, P.; Lu, Y.; Gao, X.; Liu, R.; Zhang-Negrerie, D.; Shi, Y.; Wang, Y.; Wang, S.; Gao, Q. *Chem. Commun.* **2013**, *49*, 2421.

(24) Li, H.; Gao, X.; Liu, R.; Wang, Y.; Zhang, M.; Fu, Z.; Mi, Y.; Wang, Y.; Yao, Z.; Gao, Q. *Eur. J. Med. Chem.* **2015**, *101*, 400.

(25) Möker, J.; Thiem, J. *Eur. J. Org. Chem.* **2009**, *2009*, 4842.

(26) Hartinger, C. G.; Nazarov, A. A.; Ashraf, S. M.; Dyson, P. J.; Keppler, B. K. *Curr. Med. Chem.* **2008**, *15*, 2574.

(27) Patra, M.; Johnstone, T. C.; Suntharalingam, K.; Lippard, S. J. *Angew. Chem., Int. Ed.* **2016**, *55*, 2550.

(28) Pohl, J.; Bertram, B.; Hilgard, P.; Nowrousian, M. R.; Stüben, J.; Wießler, M. *Cancer Chemother. Pharmacol.* **1995**, *35*, 364.

(29) Gynther, M.; Ropponen, J.; Laine, K.; Leppänen, J.; Haapakoski, P.; Peura, L.; Järvinen, T.; Rautio, J. *J. Med. Chem.* **2009**, *52*, 3348.

(30) Barros, L. F.; Bittner, C. X.; Loaiza, A.; Ruminot, I.; Larenas, V.; Moldenhauer, H.; Oyarzún, C.; Alvarez, M. *J. Neurochem.* **2009**, *109*, 94.

(31) Park, J.; Lee, H. Y.; Cho, M.-H.; Park, S. B. *Angew. Chem., Int. Ed.* **2007**, *46*, 2018.

(32) Pavan, B.; Dalpiaz, A.; Ciliberti, N.; Biondi, C.; Manfredini, S.; Vertuani, S. *Molecules* **2008**, *13*, 1035.

(33) Battaglia, G.; La Russa, M.; Bruno, V.; Arenare, L.; Ippolito, R.; Copani, A.; Bonina, F.; Nicoletti, F. *Brain Res.* **2000**, *860*, 149.

(34) Speizer, L.; Haugland, R.; Kutchai, H. *Biochim. Biophys. Acta, Biomembr.* **1985**, *815*, 75.

(35) Hassanein, M.; Weidow, B.; Koehler, E.; Bakane, N.; Garbett, S.; Shyr, Y.; Quaranta, V. *Mol. Imaging Biol.* **2011**, *13*, 840.

(36) Abe, H.; Murayama, D.; Kayamori, F.; Inouye, M. *Macromolecules* **2008**, *41*, 6903.

(37) Venkateswara Rao, B.; Dhokale, S.; Rajamohanan, P. R.; Hotha, S. *Chem. Commun.* **2013**, *49*, 10808.

DOI: 10.1021/jacs.6b06937
J. Am. Chem. Soc. 2016, 138, 12541−12551

(38) Quagliotto, P.; Viscardi, G.; Barolo, C.; D'Angelo, D.; Barni, E.; Compari, C.; Duce, E.; Fisicaro, E. *J. Org. Chem.* **2005**, *70*, 9857.
(39) Summa, N.; Schiessl, W.; Puchta, R.; van Eikema Hommes, N.; van Eldik, R. *Inorg. Chem.* **2006**, *45*, 2948.
(40) Roslund, M. U.; Tähtinen, P.; Niemitz, M.; Sjöholm, R. *Carbohydr. Res.* **2008**, *343*, 101.
(41) Du, Y.; Kong, F. *J. Carbohydr. Chem.* **1996**, *15*, 797.
(42) Nepogodev, S. A.; Pakulski, Z.; Zamojski, A.; Holst, O.; Brade, H. *Carbohydr. Res.* **1992**, *232*, 33.
(43) Miethchen, R.; Holz, J.; Prade, H.; Liptak, A. *Tetrahedron* **1992**, *48*, 3061.
(44) Degenstein, J. C.; Murria, P.; Easton, M.; Sheng, H.; Hurt, M.; Dow, A. R.; Gao, J.; Nash, J. J.; Agrawal, R.; Delgass, W. N.; Ribeiro, F. H.; Kenttämaa, H. I. *J. Org. Chem.* **2015**, *80*, 1909.
(45) Zhang, D.; Wang, Y.; Dong, L.; Huang, Y.; Yuan, J.; Ben, W.; Yang, Y.; Ning, N.; Lu, M.; Guan, Y. *Cancer Sci.* **2013**, *104*, 1690.
(46) Deng, S. M.; Zhang, W.; Zhang, B.; Chen, Y. Y.; Li, J. H.; Wu, Y. W. *PLoS One* **2015**, *10*, e0129028.
(47) Yamada, K.; Brink, I.; Bissé, E.; Epting, T.; Engelhardt, R. *J. Dermatol.* **2005**, *32*, 316.
(48) Ong, L.-C.; Jin, Y.; Song, I.-C.; Yu, S.; Zhang, K.; Chow, P. K.; et al. *Acta Radiol.* **2008**, *49*, 1145.
(49) Park, S. G.; Lee, J. H.; Lee, W. A.; Han, K. M. *Nucl. Med. Biol.* **2012**, *39*, 1167.
(50) Arafa, H. M. M. *Eur. J. Pharmacol.* **2009**, *616*, 58.
(51) Oliveri, V.; Giuffrida, M. L.; Vecchio, G.; Aiello, C.; Viale, M. *Dalton Trans* **2012**, *41*, 4530.
(52) Wang, Q.; Huang, Z.; Ma, J.; Lu, X.; Zhang, L.; Wang, X.; George Wang, P. *Dalton Trans.* **2016**, *45*, 10366.
(53) Young, C. D.; Lewis, A. S.; Rudolph, M. C.; Ruehle, M. D.; Jackman, M. R.; Yun, U. J.; Ilkun, O.; Pereira, R.; Abel, E. D.; Anderson, S. M. *PLoS One* **2011**, *6*, e23205.

DOI: 10.1021/jacs.6b06937
J. Am. Chem. Soc. 2016, 138, 12541−12551